Comparing 26S Proteasome Efficiency Between Long-Living and Short-Living Rodents

by
Lynda M. Bradley

A THESIS

submitted to

Oregon State University

University Honors College

in partial fulfillment of
the requirements for the
degree of

Honors Baccalaureate of Science in Biochemistry and Biophysics
(Honors Scholar)

Presented September 3, 2015
Commencement June 2016

AN ABSTRACT OF THE THESIS OF

Lynda M. Bradley for the degree of Honors Baccalaureate of Science in Biochemistry and Biophysics presented on September 3, 2015. Title: Comparing 26S Proteasome Efficiency Between Long-Living and Short-Living Rodents

Abstract approved: _____

Viviana Pérez

Many people die yearly worldwide due to diseases associated with aging, and if the process of aging in humans was more understood, the health of these patients could be improved. While many biochemical actions are involved with the aging process, loss of proteostasis has been called one of the most important causes of aging. When proteostasis is lost, proteins in the cells cannot be properly checked for quality, and build-up of toxic protein can occur. The 26S proteasome is a mechanism of proteostasis, degrading improperly folded proteins before they become toxic to the cell. While the exact mechanisms are known for how the 26S proteasome affects aging in short-living mammals, it is not well-known how it affects aging in long-living mammals. A comparative biology approach was used for this project, where a traceable 26S proteasome cellular signal was used to compare the efficiencies of the proteasome between naked mole rats, a long-living species, and mice, a short-living species. It was hypothesized that naked mole rats have a higher 26S proteasome efficiency than mice, and the aim of this study was to quantify that difference. Problems with methods and mouse cell lines made it so final comparative efficiencies could not be made between naked mole rats and mice, but protocols were refined and optimized. The end result of this project is a proposed protocol that is likely to gain data relevant to the project's aim.

Key Words: aging, proteostasis, 26S proteasome, ubiquitin, fusion proteins, naked mole rat, fluorescent quantification

Corresponding e-mail address: lynda.bradley93@gmail.com

Comparing 26S Proteasome Efficiency Between Long-Living and Short-Living Rodents

by
Lynda M. Bradley

A THESIS

submitted to

Oregon State University

University Honors College

in partial fulfillment of
the requirements for the
degree of

Honors Baccalaureate of Science in Biochemistry and Biophysics
(Honors Scholar)

Presented September 3, 2015
Commencement June 2016

Honors Baccalaureate of Science in Biochemistry and Biophysics project of Lynda M. Bradley presented on September 3, 2015.

APPROVED:

Viviana Pérez, Mentor, representing Biochemistry and Biophysics

Tory Hagen, Committee Member, representing Biochemistry and Biophysics

Kari Van Zee, Committee Member, representing Biochemistry and Biophysics

Toni Doolen, Dean, University Honors College

I understand that my project will become part of the permanent collection of Oregon State University, University Honors College. My signature below authorizes release of my project to any reader upon request.

Lynda M. Bradley, Author

TABLE OF CONTENTS

SECTION	PAGE
INTRODUCTION: BACKGROUND	1
PROTEIN AGGREGATION AND AGING	1
COMPARATIVE BIOLOGY	2
THE 26S UBIQUITIN-PROTEASOME SYSTEM	3
UBIQUITIN FUSION DEGRADATION (UFD) SIGNAL	4
HYPOTHESIS AND EXPERIMENTAL DESIGN	5
METHODS	6
RESULTS AND DISCUSSION	9
CELLULAR CULTURING	9
PLASMID PRODUCTION	9
26S PROTEASOME INHIBITION ASSAY	10
HIGH CONTENT IMAGING	12
WESTERN BLOT EXPERIMENTS	14
STABLE TRANSFECTIONS	17
CONCLUSIONS AND FUTURE DIRECTIONS	18
ACKNOWLEDGMENTS	20
REFERENCES	21

Introduction

Protein Aggregation and Aging

Though all people eventually die, not all people die from the same age-related causes. Aging itself is not a disease, but age is unfortunately one of the biggest risk factors for many diseases that kill Americans every year, including cardiovascular disease, cancers, and neurodegenerative diseases such as Alzheimer's disease ((Niccoli & Partridge, 2012)). Cardiovascular diseases and cancers were the biggest causes of death in 2010, combined killing over 1 million Americans, and Alzheimer's disease killing about 85,000 Americans ("Leading causes of death"). Given that these diseases are so lethal, it is important to not just find a cure for them but to understand how the processes of aging influence these diseases.

However, it is difficult to isolate just a few mechanisms that control aging related disorders. Instead, focusing on biological "sectors" of mechanisms that affect aging help shed light on specific diseases or aging phenotypes. One group of mechanisms that has been shown to be highly involved in the aging process is proteostasis (López-Otín, Blasco, Partridge, Serrano, & Kroemer, 2013), seen in Figure 1.

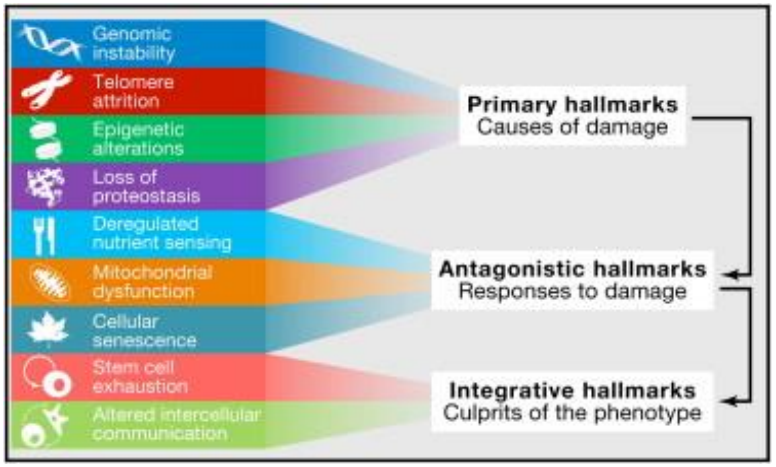

Figure 1: The hallmarks of aging (López-Otín *et al*, 2013)

Proteostasis acts to keep a balance of properly functioning and malfunctioning proteins within the cells (Powers, Morimoto, Dillin, Kelly, & Balch, 2009). The proper function of a protein is extremely dependent on its structure—the structure of a protein dictates its function. Proteins can often malfunction in the cell when they are improperly "folded", caused by an abnormal three dimensional shape within the protein's tertiary or quaternary structure. Misfolding of proteins often exposes hydrophobic regions on the protein that are normally located on the inner surfaces of a protein. When many of these surfaces become uncovered during misfolding, the misfolded proteins' hydrophobic surfaces are extremely likely to stack together. These stacks of misfolded proteins are often called aggregates, and are very energetically favorable, as seen in Figure 2. Since the aggregates are so stable, they are nearly irreversible in the cell. While aggregates are a classic sign of neurodegenerative disease, they are not the most toxic outcome of misfolded proteins. Amyloid fibrils can form, a more organized and stackable version of aggregates. These quickly can become very toxic to the cell due to their "sticky" nature (Treusch, Cyr, & Lindquist, 2009).

However, proteostasis can correct the misfolded proteins before they become insoluble aggregates—it is a preventative measure against future toxic protein formations. The main

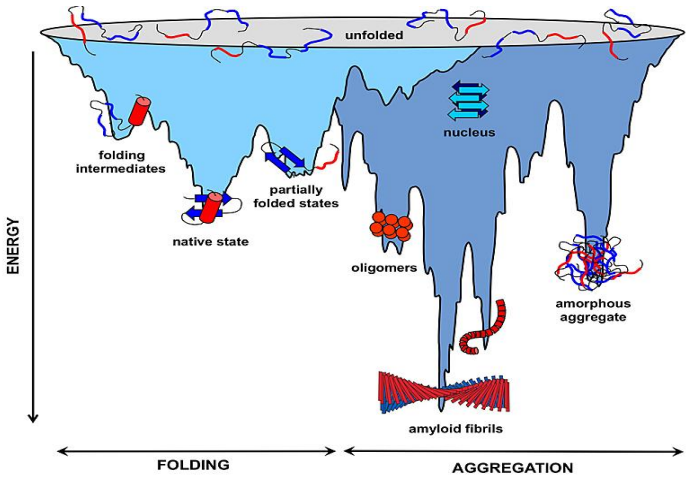

Figure 2: Energy well depicting different folding states of proteins and aggregates (Vabulas *et al*, 2015)

cellular protein quality control mechanisms utilized by proteostasis are stabilization of proteins through chaperone mediated responses, and degradation of proteins through the proteasome and autophagy/lysosomes (López-Otín, Blasco, Partridge, Serrano, & Kroemer, 2013). Several aged animal models have be found to have lowered proteasomal, autophagic, and chaperone mediated activities (López-Otín, Blasco, Partridge, Serrano, & Kroemer, 2013). Transgenic mice have shown that lifespan and healthy years are increased when certain chaperone mediated responses, autophagic activities and proteasomal activities are overexpressed. These experiments have identified specific pathways and reactions that are important to the aging process, but only in short-lived animals, such as C. elegans, yeast, and somewhat in mice (López-Otín, Blasco, Partridge, Serrano, & Kroemer, 2013). However, these proteostatic mechanisms are not well understood in long-living species.

Comparative Biology

Therefore, in order to determine the role of these proteostatic mechanisms in long-living mammals, it is beneficial to compare these mechanisms between well-known short-living species and long-living species. Through this comparative biology approach, it will be better understood how proteostatic mechanisms affect the aging of mammals, and what protective role they play during the aging process. This can eventually give researchers more information on what processes are important for human aging, given that humans are long-living mammals. Determining the role of each in the aging process will lead to understanding the specific mechanisms in place that affect aging, eventually allowing selective treatments, pharmaceuticals, and preventative measures to be created in the hope of slowing down age-related disease and increasing healthy years lived.

Two rodents are often used for comparative biology studies. The long-living rodent selected for this study was the naked mole rat, a long-living rodent that lives up to 30 years, almost ten times what is expected based on its weight and biological classification (Rodriguez, Edrey, Osmulski, Gaczynska, & Buffenstein, 2012). The naked mole rat has already been found to have a more active 26S proteasome and robust 20S activity (Rodriguez, Edrey, Osmulski, Gaczynska, & Buffenstein, 2012). It has also already been

shown previously in our lab that naked mole rat skin fibroblasts have more active chaperone, autophagic, and 20S proteasomal mechanisms in comparison to mice. The short-living companion is a simple laboratory mouse. Other comparative biology approaches have used this anima combination in past studies (Pickering, Lehr, Kohler, Han, & Miller, 2015; Austad, 2009).

The 26S Ubiquitin-Proteasome System

The 26S proteasome is a eukaryotic compartmentalized system for degrading proteins that are misfolded, non-functional, and normal (Peth, Uchiki, & Goldberg, 2010; the proteasome Tanaka, 2013). Proteins in the cell are targeted for disposal by the proteasome through the use of a small 76 residue cellular protein, ubiquitin. An ATP dependent reaction attaches ubiquitin to a protein substrate via an internal ubiquitin lysine residue. In order to degrade the protein, multiple ubiquitins must be attached to the protein substrate. Multiubiquitylated chains are made when ubiquitin's 76th residue, a glutamine, is attached to another ubiquitin's 48th residue, a lysine (Grillari, Katinger, & Voglauer, 2006). This is illustrated in Figure 3, where the 76th residue is highlighted in red, and the 48th in blue.

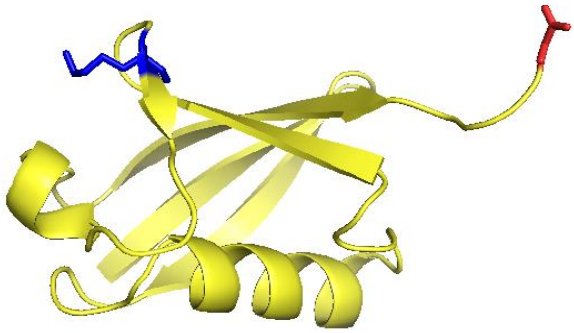

Figure 3: view of ubiquitin's essential internal lysine at site 48 (in blue) and its glutamine at site 76 (red), PDB# 1UBQ

Once the polyubiquitylated chain reaches the proteasome, it first comes into contact with the 19S cap, also known as the Regulatory Particle (RP). Seen in Figure 4, Rpn10 and Rpn13 non-ATPase subunits effectively trap the polyubiquitylated protein using their C-terminal ubiquitin-interacting motifs (UIM) and pleckstrin-like receptor for ubiquitin domains (Pru), becoming the first step in degrading the protein.

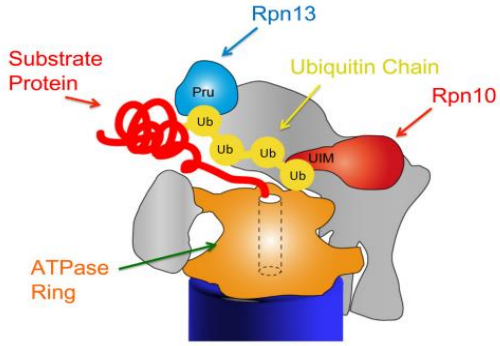

Figure 4: Cartoon depiction of integral parts of the 19S cap of the 26S proteasome (Peth *et al*, 2013)

Importantly, the next step is to remove the ubiquitins from the substrate protein—they are recycled in the cell. The enzymes that perform this task are known as deubiquitinases, and in mammalian cells are the Rpn11, Usp14, and Uch37 subunits. They cleave the ubiquitins off of the substrate protein at a site proximal to it. Continuing into the proteasome, Rpt2 and Rpt5 subunits open a "gate" which allows the substrate protein to enter a new section of the proteasome—the 20S core particle (CP).

Within the 20S core, the substrate protein will be finally degraded. This is accomplished through different rings of catalytic subunits within the core. Two outer axial stacks of α particles act to protect substrates accidentally entering the catalytic β subunits. Once the substrate reaches the β units, the protein is degraded via caspase-like, trypsin-like, and chymotrypsin-like activities that cleave peptide bonds at post-acidic, post-basic, and post-hydrophobic residues respectively.

Ubiquitin Fusion Degradation (UFD) Signal

There are several ways to signal to the proteasome that a protein needs to be degraded. The most common signaling pathway is the N-end rule, in which a protein's half-life is determined by the nature of its N-terminal protein (Mogk, Schmidt, & Bukau, 2007).

Another degradation phenomenon is also noted within engineered ubiquitin-fusion proteins, proteins that have been linked during translation via an amino acid to an ubiquitin (Johnson, Bartel, Seufert, & Varshavsky, 1992; Johnson, Ma, Ota, & Varshavsky, 1995). Johnson et. al. discovered through pulse-chase methods that fusion moieties followed a degradation pattern similar to an N-end rule where the connecting amino acid determined the half-life of the fusion protein. The group's studies were done on ubiquitin-βgal fusion proteins, as diagramed in Figure 5, where "X" represents the variable amino acid that connects the two proteins. Johnson et. al. found certain N-terminal fusion proteins that were stably de-ubiquitinated normally, including an ubiquitin fusion protein that was fused with a methionine residue.

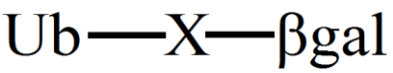

Figure 5: Diagram of *Johnson et. al.*'s fusion proteins

The group also found that when the 76th residue of ubiquitin, an essential glutamine, was changed to an alanine or a valine, the entire fusion protein was degraded by the proteasome. Changing the glutamine to a valine or alanine caused the fusion protein to be resistant to deubiquitinases, but also was still multiubiquitylated since the lysine 48 residue was available for chemistry. The half-life of this fusion protein was recorded around 4-5 minutes, and did not follow first order kinetics. The protein was found to not follow first-order kinetics due to newly produced unstable proteins being degraded more efficiently than mature ones (Johnson et al., 1995).

Dantuma et. al. were able to create a method for observing the degradation of ubiquitin fusion proteins without performing pulse-chase methods (Dantuma, Lindsten, Glas, Jellne, & Masucci, 2000). This is an advantage over Johnson et. al.'s design because radiolabeling for pulse-chase methods is fairly difficult and expensive. Dantuma et. al. fused ubiquitin to GFP, testing the effects of various connector amino acids on protein degradation rates.

Corroborating Johnson et. al.'s amino acid connector data, Dantuma et. al. found that a methionine residue connecting ubiquitin and GFP (Ub-M-GFP) was quickly deubiquitinated, evidenced by the fact that the GFP fluorescent signal was stable. If the fusion protein had been degraded, the GFP signal would decrease significantly over time,

since the GFP would also be degraded by the proteasome. Dantuma et. al also found that altering the glutamine in ubiquitin at site 76 to a valine residue and connecting it to GFP with another valine residue (Ub-G76V-GFP), the fusion protein rapidly lost fluorescence signal. This indicated that the fusion protein was indeed uncleavable by deubiquitinases. This loss in fluorescence was observed only after treating the cells containing Ub-G76V-GFP with a reversible proteasome inhibitor. Since the fusion protein was not being degraded by the proteasome, the GFP built up in the cell, increasing the fluorescence signal by 100 fold. Once the inhibitor was removed, the fluorescent signal was observed to decline due to the protein being degraded. Dantuma et. al. concluded that this was a way to observe proteasomal degradation and that Ub-G76V-GFP degradation reflected the fate of other short-lived cellular proteins, such as cyclins and p53.

Experimental Design and Hypothesis

The aim of this project was to find out if naked mole rates have a more efficient 26S proteasomal system than mice, using Dantuma et. al.'s fusion protein design. Naked mole rats have already been found to have increased proteasomal activity in comparison to mice (Pride et al., 2015), However, as previously discussed, higher proteasomal activity does not necessarily mean that proteins are cleared from the cell more efficiently, because the clearance through the 26S proteasome relies on 19S efficiency, and ubiquitinase and deubiquitinases activities. Dantuma et. al.'s UFD technique can quantify the efficiency that the 26S proteasome is able to degrade cellular proteins that are involved in aging.

The hypothesis of this project is that naked mole rats will have higher 26S proteasome efficiency in comparison to mouse 26S proteasome efficiency. Expected fluorescence data is seen in Figure 6, based on this hypothesis. Once ending MG132 treatment, Ub-M-GFP protein is expected to have a fluorescent signal that stays relatively constant over time, due to the fact that ubiquitin is cleaved, leaving only GFP within the cell. A slight decline in the fluorescent signal is expected over time due to inefficiencies of the deubiquitinases and the fact that GFP is degraded naturally in the cell over time. Once ending MG132 treatment, Ub-G76V-GFP protein in NMR is expected to be cleared significantly faster from the cell than the mouse Ub-G76V-GFP protein, causing the NMR Ub-G76V-GFP signal to decline at a much steeper rate than the mouse's.

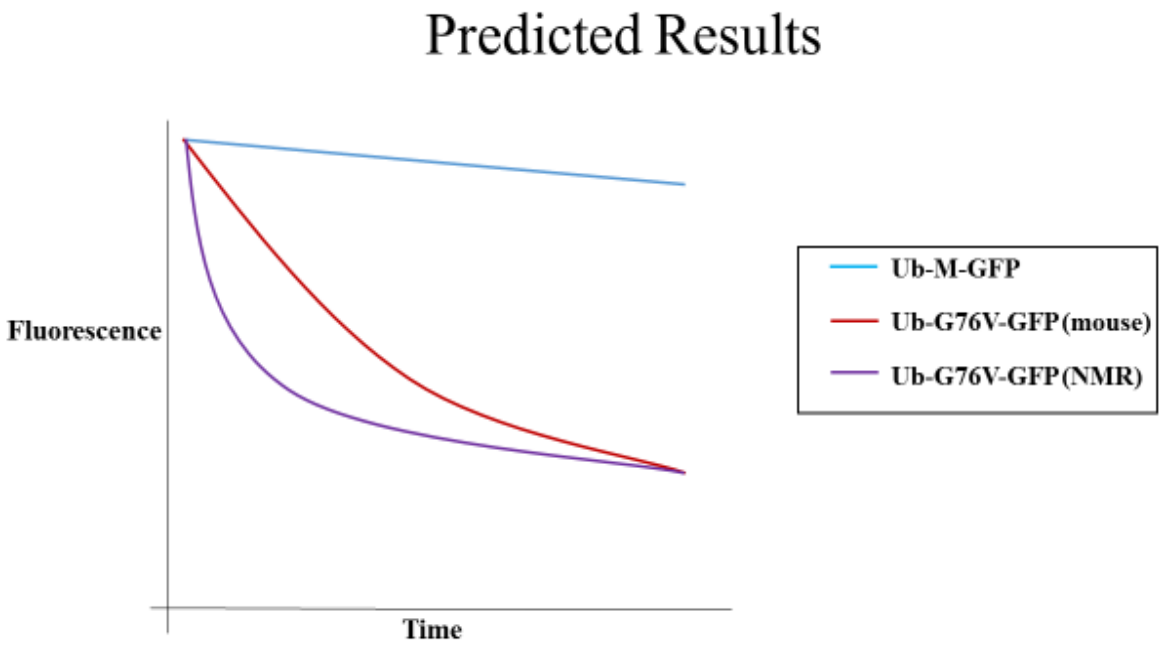

Figure 6: Expected fluorescence signal data based on hypothesis, depicting the behavior of fluorescent signals over time for the different experimental plasmids.

Methods

Cell Culturing

Naked mole rat and C57BL/6 mouse skin fibroblasts were cultured using DMEM Low Glucose, 10% fetal bovine serum, and 1% penicillin/streptomycin (complete media) in 10 cm plastic culturing dishes. C57BL/6 mouse skin fibroblasts were obtained in laboratory through control mice from other laboratory experiments. Naked mole rat fibroblasts were cultured on collagen-coated 10 cm plastic culturing dishes. Both were grown to 80% confluency before experiments were performed. Experiments done on both cell lines were performed on cells that were below passage 15.

Once desired confluency was reached, the cells were washed with DPBS and treated with warm trypsin for 5 minutes. Once the cells were detached from the dish, they were centrifuged at 193 g for 5 minutes before resuspending in appropriate amount of complete media.

Plasmids

GFP, Ub-M-GFP, and Ub-G76V-GFP plasmids conferred kanamycin resistance for E. coli production and neomycin/gentamycin (G418) resistance for selection purposes. All three also use the EGFP-N1 vector as a backbone.

Plasmid Production

Ub-M-GFP and Ub-G76V-GFP plasmids were produced using ProMega PureYield Plasmid Purification System. Transgenic E. coli were cultured for 24 hours using 50 µg/mL kanamycin and 20 g/L luria broth, then harvested at 3,000 g for 20 minutes. Further procedures were followed according to ProMega protocol. Plasmid purity and concentration were measured using NanoDrop.

Transient Transfection Protocol

Naked mole rat and mouse skin fibroblasts were transfected using FuGene lipofectamide. 26 hours before transfection, 80% confluent cells were starved with serum-free DMEM low glucose antibiotic media for 12 hours. This was done in order to synchronize cell cycles in the culture (Davis, Ho, & Dowdy, 2001). After starvation, cells were treated with complete media to allow for recovery before transfection. Transfection protocol was optimized to a 6:1 volume reagent to µg DNA mixture, using 1 µg/µL DNA. Transfection mix was incubated at room temperature for 15 minutes according to FuGene protocol before transfection, using penicillin/streptomycin free media. Both Ub-M-GFP and Ub-G76V-GFP plasmids were used in transfections as well as a positive GFP control and a negative control with no DNA. Cells incubated with the transfection in 10 cm dishes for 24 hours before media change. Successful transfections were evaluated using fluorescent 20X microscope.

20S Proteasome Inhibition Assay

Fibroblasts were homogenized in homogenization buffer (50 mM Tris-CL, pH 8.0; 1 mM EDTA; 0.5 mM DTT) and protein concentrations were measured by Bradford assay. For each sample, 100 mg total protein was assayed in triplicate in 96-well plates using a 20S proteasome fluorometric (AMC) assay kit as per instructions from the vendor (Calbiochem, Billerica, MA). Release of free AMC from the fluorogenic peptide Suc-Leu-Leu-Val-Tyr-AMC was measured over time at 37 C using a microplate fluorescence spectrophotometer. 20S activity was calculated by the slope of free AMC release over time after ~10 min period of normalization. 20S proteasome specific activity was calculated by normalizing 20S activity to the quantity of 20S proteasome as measured by Western blot; data were expressed as AMC release per second per mg of protein. A proteasome inhibitor, Lactacystin, was used to verify proteasome-driven proteolysis (Pride et al., 2015).

Flow Cytometry

Flow cytometry was done in ALS within the Cell Imaging and Analysis Facilities and Services Core. Cells were prepared for analysis by removing media, detached and resuspended in DPBS. Gate selection was set to capture cells that expressed GFP in a population more so than the autoflourescent population. Sam Bradford helped greatly with this process.

High Content Imaging

High content imaging system and MetaExpress software was used in Dr. Julie Greenwood's laboratory.

Once cells were successfully transfected, they were transferred to a black-sided 96-well plate. Three types of treatments were used: control transfected cells, transfected cells treated with 10 µM MG132 for 24 hours, transfected cells treated with 10 µM MG132, 20 mM ammonium chloride, and 100 µM leupeptin for 24 hours. MG132 was used as a reversible proteasome inhibitor and ammonium chloride/leupeptin were used as reversible autophagy inhibitors. Autophagy inhibitors will be used to determine if autophagy plays a quantifiable role in ubiquitin lost, due to studies indicating ubiquitin is sometimes terminally degraded by autophagosomes (Kraft, Peter, & Hofmann, 2010).

Half of each of the inhibitor treated cells did not have the inhibitors removed for the 48 duration of the experiment.

Western Blot Experiments

Cells were transfected in a 10 cm tissue dish using standard transfection protocol. After 24 hours and confirmation of successful transfection, cells were passed into four 1 cm dishes. After 12 hours to allow attachment of cells, dishes were treated with 10 µM MG132 for 14 hours. Wthout removing the MG132, cells were treated with 50 µg/mL of cycloheximide for 3 hours to prevent new production of the GFP fusion proteins—Dantuma et. al. hypothesized that the Ub-G76V-GFP protein was co-translationally degraded. After 3 hours, the media in all four dishes was changed, removing the MG132; the new media still contained 50 µg/mL of cycloheximide . The four 1 cm dishes were harvested using RIPA buffer and a rubber policeman after 0 minues, 15 minutes, 30 minutes, and 60 minutes. Samples were vortexed three times, separated by two minute iced incubations, then stored in -25^{o}C freezer.

Bradford duplicates were performed on supernatant and samples were normalized for Western blot analysis. Samples were run on a 4-12% gradient acrylamide gel and mouse samples were re-run on a 12% acrylamide gel using Precision Plus Protein Standard Kaleidoscope.

A 1:1000 dilution rabbit anti-GFP and a 1:2000 dilution mouse anti-actin primary antibody was applied to the membrane overnight at 4 ^{o}C. After PBS-T washes, appropriate secondary antibodies were applied to the membrane. Imaging was performed in the BioRad ChemiDoc Imaging System.

Stable Transfection

Successful transient transfections of naked mole rat Ub-M-GFP and Ub-G76V-GFP were treated with 50 µg/mL G418 for two and three weeks, respectively. Both plasmids had the neo gene, allowing transfected cells to survive the antibiotic treatment.

Media was removed every 3 – 5 days. Cells were then washed with DPBS, and media containing G418 was replaced. Once many cells detached and transfection efficiency was >50%, antibiotic was removed.

Results and Discussion

Cellular Culturing

Naked mole rat fibroblasts were usually fully cultured to 80% confluency within 5 days of beginning culture from liquid nitrogen stock. Colonies produced had minimal abnormalities or media debris, and this was consistent over three animals.

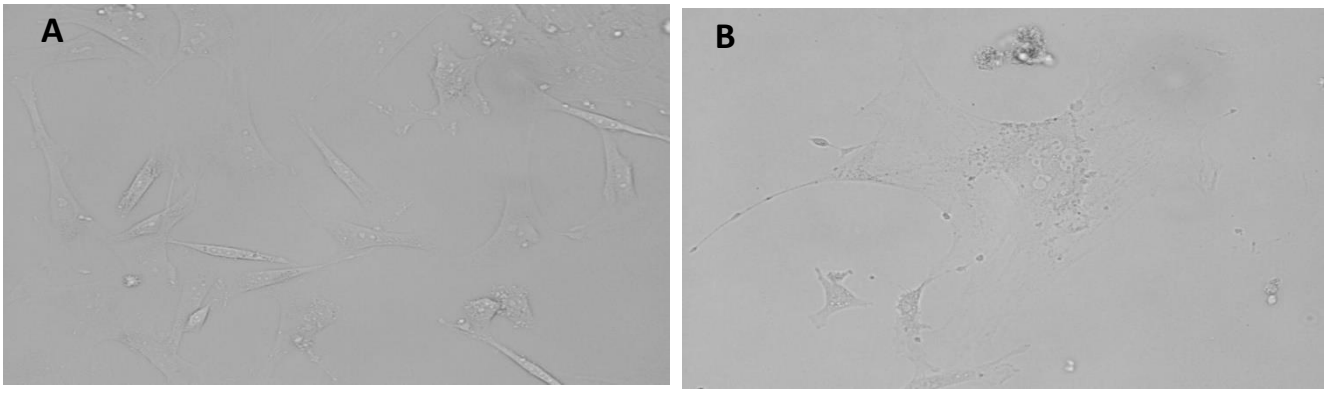

Mouse skin fibroblast wt#1 Mouse skin fibroblast wt#5

Figure 7: Photographs of normal mouse skin fibroblast morphology, seen in A as an image of wt#1, and abnormal morphology, seen in B as an image of wt#5

Mouse fibroblasts did not culture as easily. Many cell lines from different animals did not grow well, had abnormal morphology, and had a lot of media debris. Many months of testing cells led to the discovery that at least one cell line was viable, the wt #1 line. 20X images highlighting the differences in morphology between a representative abnormal cell line, wt #5, and the normal wt #1 are seen in Figure 7. Wt#1 has easily distinguished cellular boundaries, is not stretched out very much, has minimal cellular debris and unusual black dots/vacuoles within the cells. Wt#5 appears to be very stretched out, and has lots of small, dark debris and vacuoles that are not due to bacterial infection, including mycoplasma contamination (mycoplasma data not shown)

Plasmid Production

Ub-M-GFP and Ub-G76V-GFP plasmids purified using the PureYield system had results as seen in Table 1.

Plasmid	Concentration (ng/µL)	A_{260}/A_{280}
Ub-M-GFP	523.6 ±0.3	1.93
Ub-G76V-GFP	388.7 ±0.1	1.90

Table 1: Plasmid purity data

The plasmids were deemed appropriate to use in experiments, due to reasonably high concentrations for the experiments to be done and A260/A280 purity ratios over 1.80.

20S Proteasome Inhibition Assay

Proteasome inhibition by MG132 was measured over 48 hours to check that the proteasome was sufficiently inhibited. As seen in Figure 8, percent inhibition of the 20S proteasome was measured. Lactacystin is the positive, irreversible 20S proteasome inhibitor, which is why its inhibition levels for both mouse and naked mole rat are nearly 100%. 10 µM MG132 was selected as the experimental concentration of MG132 since it inhibits both mouse and naked mole rat 20S proteasomes as least ~40%, and was not toxic to cells ove 48 hours (viability data not shown). 10 µM MG132 is also commonly used in literature (or an even lower concentration), including on HeLa cells and mouse embryonic fibroblasts (Dantuma et al., 2000; Santiago-Josefat, Pozo-Guisado, Mulero-Navarro, & Fernandez-Salguero, 2001). As seen in the data, 10 µM MG132 inhibits the mouse and naked mole rat cells' proteasomes differently. Due to this difference, data used for 26S proteasome efficiency comparisons was expressed in ratios within the animal.

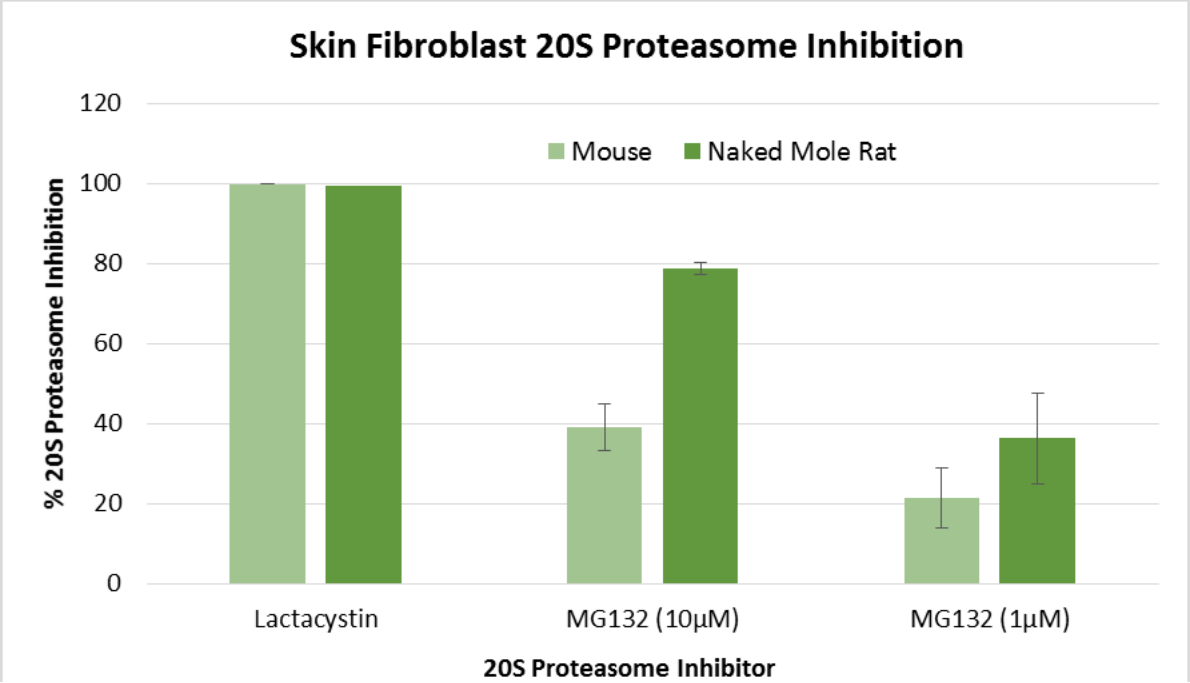

Figure 8: 20S proteasome inhibition assay results, with mouse data seen in the light green, and naked mole rat data seen in the darker green

Transient Transfections and Flow Cytometry

Transfections qualitatively worked most efficiently and precisely both in naked mole rat and mouse fibroblasts at a 6:1 FuGene to DNA ratio. This was tested over the course of over 10 transfections. Transfections were more efficient in naked mole rat fibroblasts compared to mouse fibroblasts, a phenomenon that was observed by other laboratory workers with different plasmids. This observation was independent of transfection mix

(mix was made in same tube for both cell lines), incubation time, confluency, temperature, passage number, and relative cell health.

Realizing early on that the transient transfections were not as efficient as desired for experiments, it was decided to try to separate the fluorescent cells from non-transfected cells in order to run experiments with many fluorescent cells. While not enough fluorescent cells were collected for an experiment, valuable information about the transient transfections. While many transfection efficiencies in naked mole rats visually appeared to be reasonable when examined under a fluorescent microscope, flow cytometry showed a different result. For a naked mole rat Ub-M-GFP transfection that appeared to be about ~30%, it appeared that only 3.68% of "counted particles" were actually GFP fluorescent. 3.68% efficiency is extremely poor—however, this is probably not very accurate, and the visual assessment might be more accurate. When the flow cytometer "counts the particles", it counting anything that is in the same shape/size as a cell. Therefore, cellular debris, media impurities, and other objects can be counted as cells. The transfection efficiency was not worrisome in the mind of the flow cytometer technician.

As seen in image A of Figure 9, it is seen that there are two fairly distinct populations—a large peak that represents cells that are autoflourescent and those that are transfected, expressing GFP. However, the peak is fairly broad and right-shifted, meaning that there are many cells that vary in how much plasmid they are expressing. This might indicate that serum starvations do not perfectly set the cellular cycles.

A figure representing the "top-down" view these populations is seen in image B of Figure 9. If one could imagine image A being a side-on view of populations of cells, image B is the top-down view of the same populations. The R3 gate surrounds the same population circled in red in the image on the left. The closer the colors in the image below get towards the blue end of the spectrum, the higher the concentration of cells in that area is.

The transfection efficiency for the Ub-G76V-GFP was lower at 1.02%. Seen in image A of Figure 10, it interestingly did not have two clean peaks like the Ub-M-GFP did, but instead had three: an autoflourescence peak and two transfection peaks, circled in red. The largest population of transfected cells is also just a shoulder on the autoflourescence peak, indicating that most of the cells were faintly fluorescent. The second transfected peak had an extremely small population but appeared to be brighter. These results show that the serum free starvations are not able to synchronize the cells well, since the cells are at many various stages of degrading the Ub-G76V-GFP protein. If the fusion protein was being

degraded at the same time, the flow cytometry would show a sharp, relatively thin peak all at one level of fluorescent brightness.

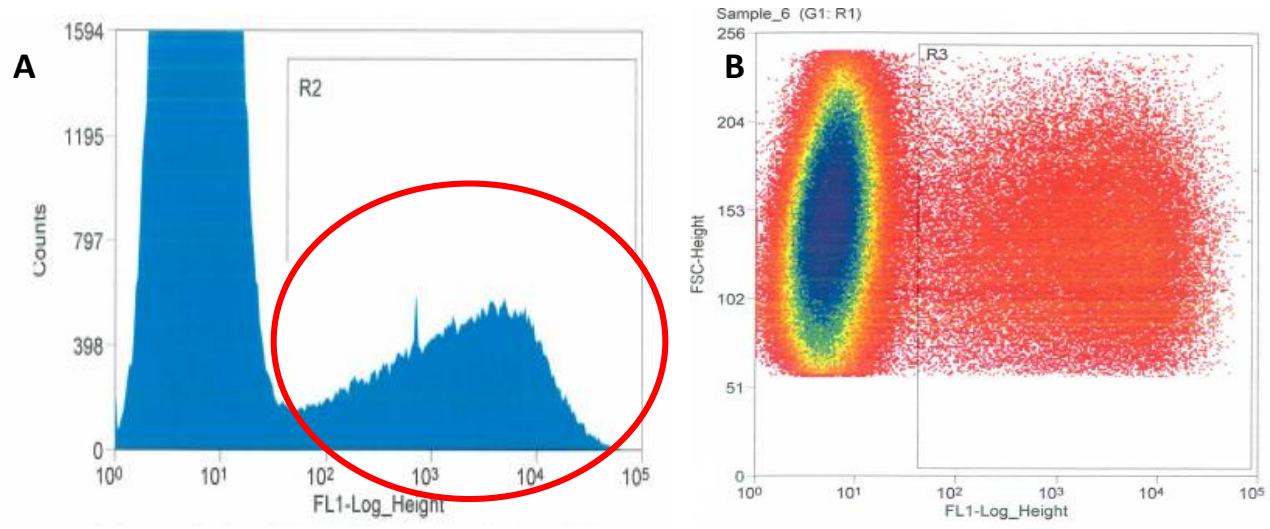

Figure 9: Flow cytometry results for Ub-M-GFP transient transfection. Image A shows population over fluorescence intensity, and Image B is a top-down view of the left-hand image, where blue represents a very dense population of cells

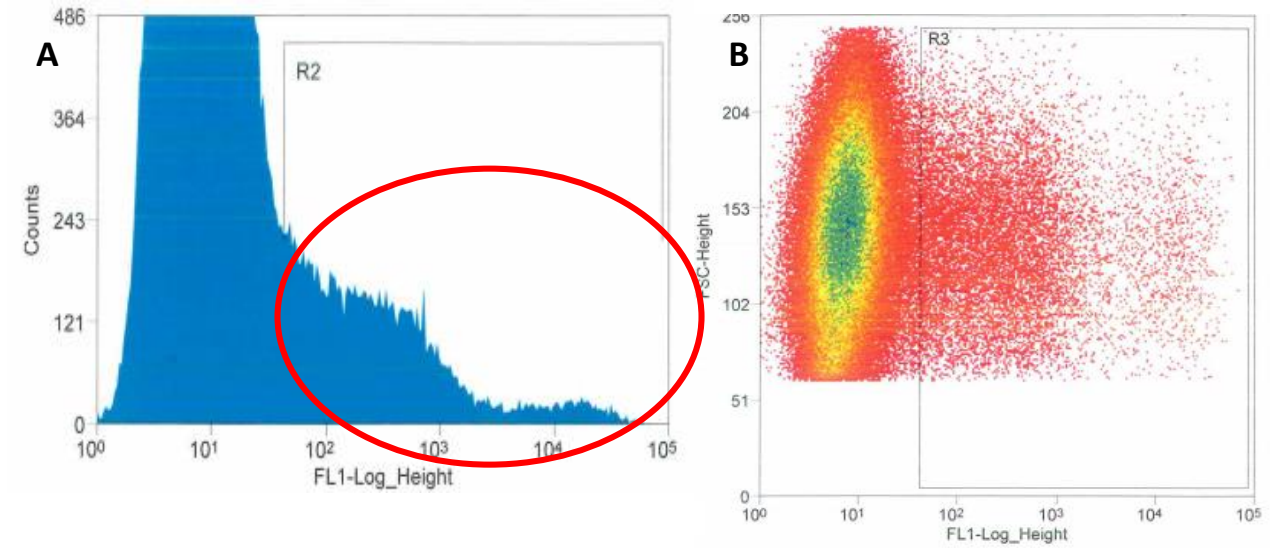

Figure 10: Flow cytometry results for Ub-G76V-GFP transient transfection. Image A shows population over fluorescence intensity, and Image B is a top-down view of the left-hand image, where blue represents a very dense population of cells

High Content Imaging

Once transient transfections were optimized, it was desired to learn more about the decline of Ub-G76V-GFP protein over a long period of time- 48 hours. Unfortunately, the data from high content imager were inconclusive. When viewing the same cells over the course of 36-48 hours, there appeared to be no trend of fluorescence increase or decrease in individual cells. From watching many cells over time, it became very apparent that they

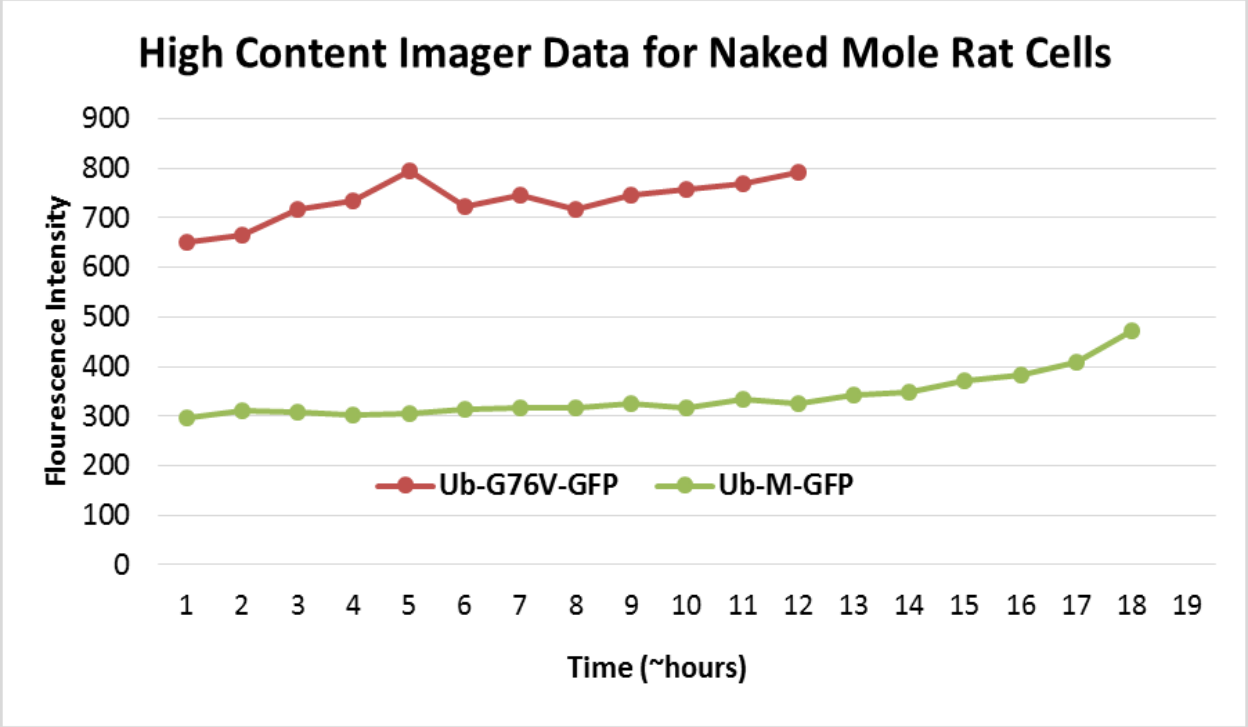

Figure 11: Quantification of high content imager data using MetaExpress, showing the change in fluorescent intensities of a single cell over time.

were not synchronized properly. Some would begin to express GFP while others began to lose GFP or die. While quantifying fluorescence intensity over time, it mostly followed a somewhat sinusoidal trend before peaking dramatically as the cells collapsed and died. This was seen rather universally over all treatments and both plasmids. Some examples of this are seen in Figure 11.

This type of data collection proved to be ineffective for several reasons. Firstly, the time in-between data points might have been too long to capture the production and decline of the experimental Ub-GFP Also during each time point, the cells could be producing the fusion proteins at about the same rate they are being degraded leading to data that would appear to not change significantly over time. Secondly, some cells died very quickly during the experiment, indicating that the plates were too confluent to support all of the cells. However, having the plates that confluent were necessary in order to have enough green cells per well. Thirdly, the cells were not well synchronized, which made analyzing a few cells over time not reflect the average rise and decline in fluorescence well, defeating the purpose of using the high content imager. Lastly, the MetaExpress software was incredibly

tedious and difficult to use for this purpose. The data over 48 hours in 96 wells mostly needed to be analyzed manually, and even then the software was often unable to distinguish between cells, debris, and dying cells. Therefore, after a few experiments to confirm these trends, this method of data analysis was discontinued.

Western Blot Experiments

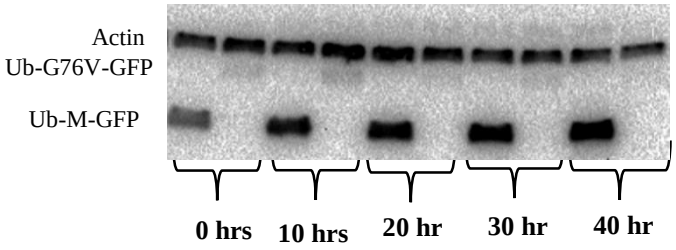

Figure 12: Western blot results for 40 hr experiment on naked mole rat cells after treatment with MG132

Since the high content imager experiments did not represent the average protein degradation well, it was decided that a western blot experiment would be able to paint a better picture of Ub-G76V-GFP decline. First western blot experiment on naked mole rat cells showed that Ub-G76V-GFP and Ub-M-GFP can be separated on a membrane. As seen in Figure 12, Ub-M-GFP bands are the lowest bands. Actin bands are located on the top, and Ub-G76V-GFP bands are located just underneath actin bands. While faint, it appears there is a set of bands just below actin protein, which is believed to be low amounts of Ub-G76V-GFP. When Ub-M-GFP is deubiquitinated, it appears to lose about ~8-10 kDa of ubiquitin,

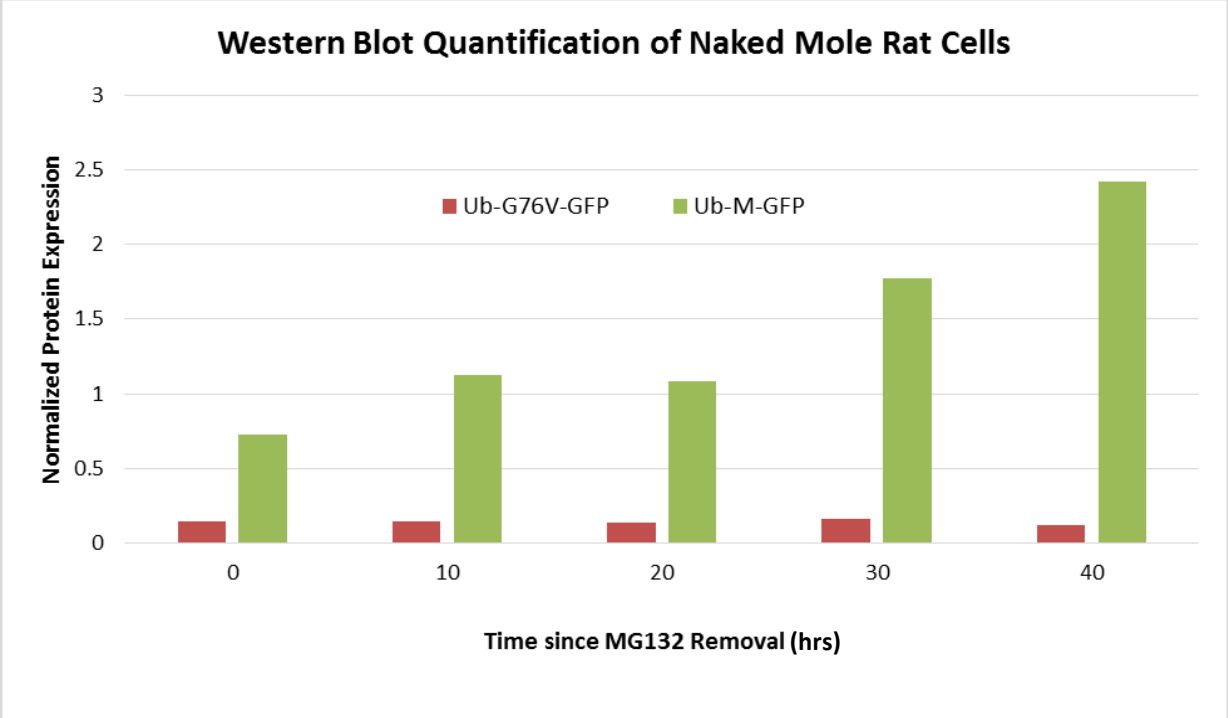

Figure 13: Quantification using ImageLab of Figure 13. Ub-M-GFP data is seen in green, and Ub-G76V-GFP data is seen in red

which remains on the G76V protein. This small size difference allows for separate quantification of bands. Quantification using Image Lab 4.0 is seen in Figures 13 and 14.

In Figure 13, quantification confirms that there are low levels of UbG76V-GFP protein. As seen by the small red bars, the expression levels of Ub-G76V-GFP are much lower than expression levels of Ub-M-GFP. This is surprising, especially given that initial levels of Ub-G76V GFP are not very high in comparison to Ub-M-GFP. According to Dantuma et. al., the detectable level of Ub-G76V-GFP should be much higher. This lack of build-up could be caused by the lack that not enough cells were transfected with the Ub-G76V-GFP plasmid, or that the protein just does not build-up as much in the cell as Ub-M-GFP. Ub-M-GFP levels were as expected, rising slowly over time as the cleaved GFP protein accumulated in the cell. A scaled version of the Ub-G76V-GFP protein expression levels in naked mole rats is seen in Figure 14. As easily seen, there is not a trend of decline or

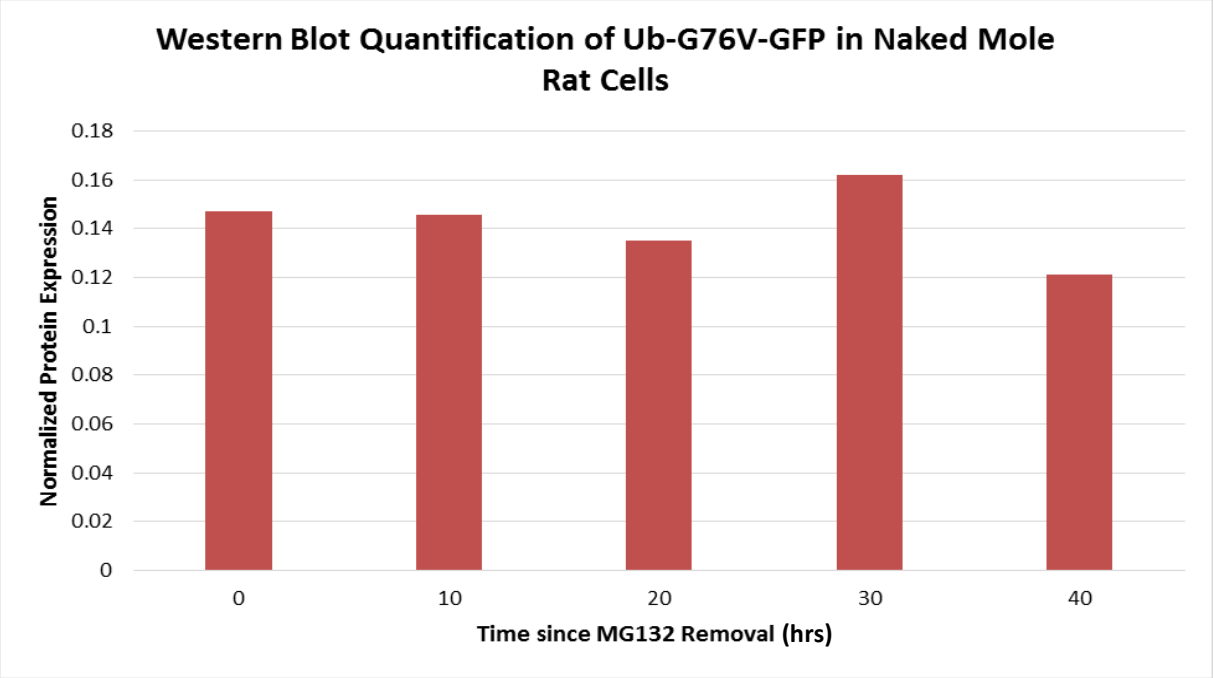

Figure 14: A zoomed-in view of the Ub-G76V-GFP data seen previously in Figure 14

increase in the protein at selected time points. This indicates that the ubiquitin fusion proteins are created and destroyed in a much shorter time than 10 hours, even after MG132 treatment. In order to avoid issues with creating more Ub-G76V-GFP protein while the decline is attempting to be measured, a new experiment had to be designed that would stop translation of the plasmid.

Translation was halted in the next western blot experiment through pre-treatment with cycloheximide, since cycloheximide does not inhibit protein degradation (Feldman & Yagil, 1969; Zhang et al., 2007). This experiment had different harvesting times—much shorter to account for the short half-life of Ub-G76V-GFP according to the literature. Seen in Figure 15, naked mole rat samples for 0, 15, 30, and 60 minutes showed up well for both

Ub-M-GFP and Ub-G76V-GFP. However, only faint, thin bands were seen for mouse Ub-M-GFP samples after overexposing the membrane for 130 seconds (not shown). When the mouse samples were run at a higher concentration on a separate membrane, Ub-M-GFP bands were visible, but no Ub-G76V-GFP bands appeared and the actin bands became extremely overexposed from the high protein levels (not shown). This confirms previous visual data that indicated mouse cells did not transfect as efficiently as naked mole rats. The actin bands appear to be relatively equal, indicating that proper amounts of protein were loaded onto the gel. Therefore, the reason why no true bands appear on the mouse blot is because they have small amounts of GFP—yet another issue with transient transfections.

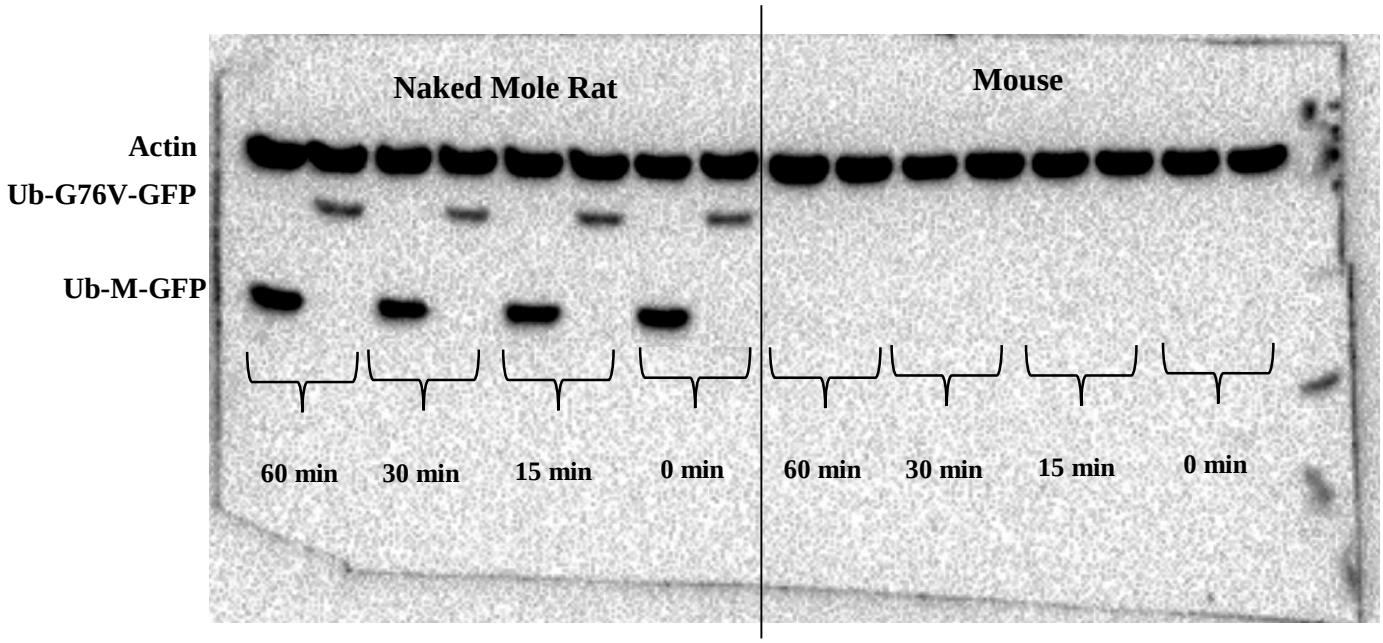

Figure 15: Western blot results for 60 minute experiment using naked mole rat and mouse cells pre-treated with cycloheximide and MG132

Quantification of Figure 15 revealed that the levels of both Ub-GFP proteins did not vary much, as seen in Figure 16. This indicates that the times selected for the experiment were too close together, and in the future will need to be further apart. The levels at the experimental time points were expected to show a decline, since the half-life of the protein was only ~4-5 minutes (Johnson et al., 1995). However, this was in S. cerevisiae, and the half-lives could be very different in rodent cells. More Western blot experiments must be conducted at different time points to determine approximate half-lives.

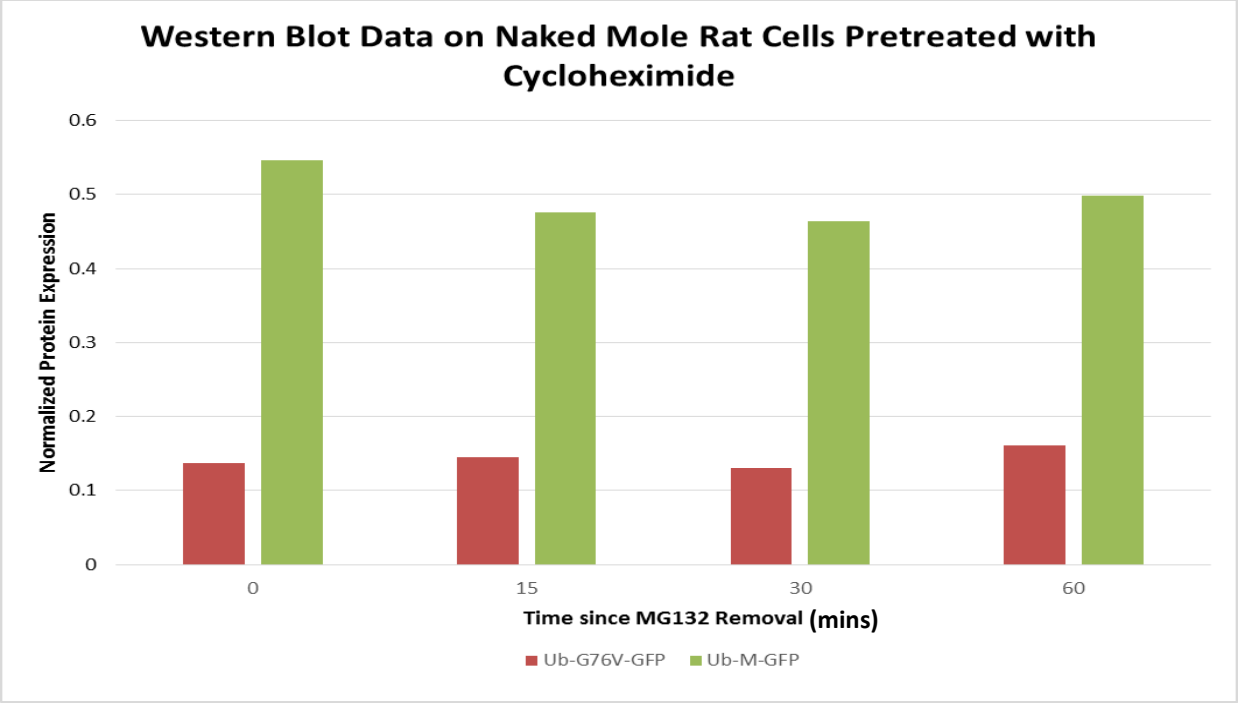

Figure 16: Quantification of Western Blot data in Figure 15. Ub-M-GFP data is seen in green and Ub-G76V-GFP data is seen in red.

Stable Transfections

In order to alleviate issues that arise from using transient transfection, such as poor efficiencies, too little fluorescent cells, failure to transfect, and the expense of transfection reagent, stable transfections of both plasmids were made in naked mole rat cells.

A Ub-M-GFP stable transfection was produced fairly easily in naked mole rat cells after two weeks of treatment with G418. Ub-G76V-GFP stable transfections were produced after three weeks of treatment. Colonies formed shortly after. Ub-M-GFP colonies were able to be photographed at 20X, but colonies could not be photographed at 10X. Due to a lack of synchronization, fluorescent colonies in the Ub-G76V-GFP stable transfections were too faint to be imaged. An image of a fluorescent Ub-M-GFP colony are seen in image B of Figure 18, with the Brightfield image for comparison in image A in Figure 17. These images show that the colonies produced from G418 treatment successfully incorporated the plasmid. It is estimated that the same percent incorporation is present in Ub-G76V-GFP, though it is not shown here. The Ub-G76V-GFP plasmid still needs to be treated with MG132 in order to have cells that are fluorescent enough to be photographed. Upon visual examination in the fluorescent microscope, it is seen that the Ub-G76V-GFP transfections are stable, but unfortunately the fluorescent signal is too faint to be photographed properly.

The stable transfections produced will be used for future experiments, so that there is no worries about efficiencies in transient transfections. Once proper mouse cell lines are established, a stable transfection will be made with them as well.

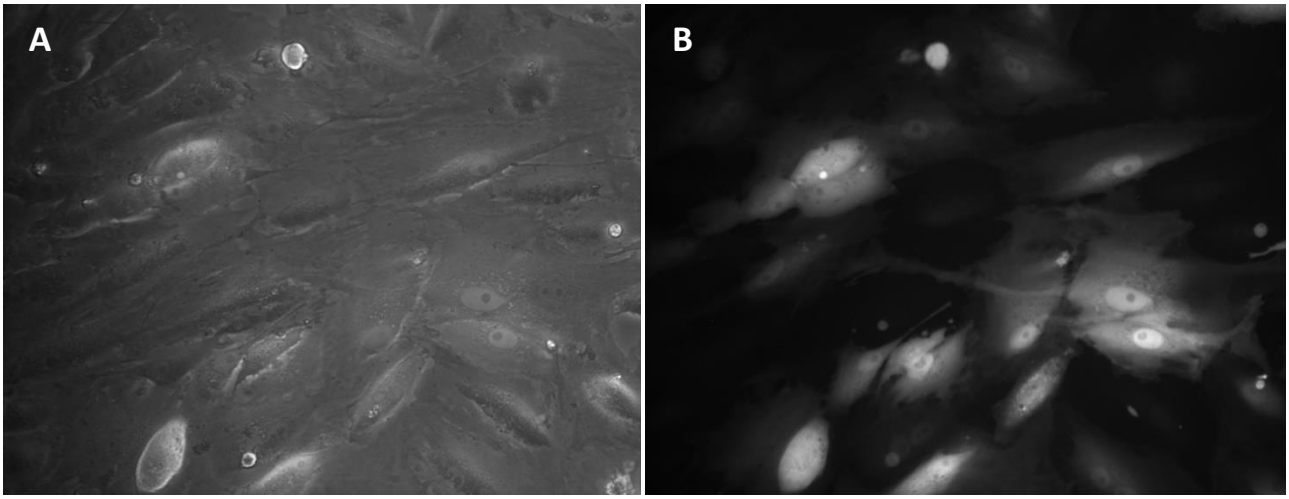

Figure 17: Images of stable Ub-M-GFP colony in naked mole rat cells. The left-hand image is a Brightfield photograph of the colony, and the right-hand image is a fluorescent photograph of the colony

Conclusions and Future Directions

The objective of this research project was to compare 26S proteasomal rates between naked mole rats and mice in order to better understand how the rate of proteasomal degradation could potentially be involved in healthy aging. A system of GFP fluorescent ubiquitin fusion proteins were intended to quantify the 26S proteasome rates, with Ub-G76V-GFP degradation rates comparable to other small cellular proteins that are involved with aging. However, many experimental method and data collection issues were encountered. Most of this project was spent troubleshooting methods and data collection. However, this project can continue once I graduate because specific parameters and data collection methods were investigated and narrowed down.

Using flow cytometry, it was discovered that the cells were not well synchronized by serum starving, and will need to be synchronized chemically in the future. In addition, once they are chemically synchronized, they should be checked for synchronization by measuring p16 and cyclin expression. After using the high content imager, it was realized that no decline would be able to be viewed if the cells could produce the fusion proteins while they were being degraded, and that cycloheximide must be used. Through western blot experiments, the times of time points necessary to conduct experiments was investigated, and a much narrower time frame and time spacing was developed. It was also discovered that western blotting is the proper way to measure both fusion proteins. Next time a western blot experiment is performed, proposed time points would be 0 minutes, 1 hour, 2 hours, 4

hours, and 6 hours. In order for the project to continue and actual comparative biology data to be gained, new mouse skin fibroblasts must be harvested—and conveniently enough, new C57BL/6 WT mouse cells will be ready within a month. Once transfections are performed successfully on mouse cells, based on previous data from our lab, the transfection efficiency should be about ~40%, and stable transfections can be made. Though no comparison between mice and naked mole rats could be done before the end of this project, information about methods was gained. And of course, if this project gets meaningful data, the same experiments can be performed with other types of mammals that are short and long living, such as marsupials.

But why bother? Why continue to work on this project when there has been so many problems and set-backs, and experiments could just be performed directly on human cells? Why waste time with small long-living mammals when the end-goal species to study is already within reach? The point of this study is to understand how a mechanism might be important to healthy aging in long-living mammals. Even if it was found that human cells have a very high proteasomal efficiency, it just indicates that humans have high proteasomal efficiency—it does not mean that a high proteasomal efficiency is a characteristic of long-living mammals. It is important to use several species for comparative biology studies in order to confirm that a particular mechanism is important overall to a trait (Austad, 2010). Therefore, in order to map out a greater understanding of the aging process, it must be known how a mechanism affects an entire set of animals.

Acknowledgments

- To my ever patient, jovial, and supporting PI, Dr. Viviana Pérez, who I have learned a great deal about being a scientist from—I'll never thank you enough for all you've done for me!
- To my post-docs, Dr. Zhen Yu and Dr. Rong Wang, who seem to have an answer for every question I have and always helped me with my problems
- To our laboratory's graduate student, Bharath Sunchu, for being a friend, supporter, ad someone who I can bounce ideas off of. A thanks also goes out to Natalia Díaz, for helping me with my project while she was here.
- To my undergraduate companions: Kelsey Caples, Collin Ruark, and Stephanie Zhao—how would I have gotten through the long days and endless troubleshooting without you? Thanks for being my best friends.
- To Dr. Hagen, for helping guide me through the thesis process, being a mentor, and of course, agreeing to be on my committee.
- To Dr. Kari Van Zee, for being a mentor and a friend throughout my senior year, always able to give me advice, and also agreeing to be on my committee
- To graduate students Nicholas Thomas and Amanda Kelley and post-doc Dr. Kate Shay, mentors I have come to numerous times with science (and life) questions.
- To the Greenwood lab, especially John Gamble, for helping me with fluorescent imaging
- To Sam Bradford, who operated flow cytometry and gave good cell culturing advice
- To the Oregon State University Biochemistry and Biophysics department, for giving me numerous awards to continue my research, including two CURE awards and a KARE award. I would not have been able to balance a work-research life if I had not been given these awards.
- To my friends, mentors, and family who have supported me through my years of research…and edited many papers

Thank you!

References

Austad, S. N. (2009). Comparative biology of aging. The Journals of Gerontology. Series A, Biological Sciences and Medical Sciences, 64(2), 199–201. http://doi.org/10.1093/gerona/gln060

Austad, S. N. (2010). Cats, "Rats," and Bats: The Comparative Biology of Aging in the 21st Century. Integrative and Comparative Biology, 50(5), 783–792. http://doi.org/10.1093/icb/icq131

Dantuma, N. P., Lindsten, K., Glas, R., Jellne, M., & Masucci, M. G. (2000). Short-lived green fluorescent proteins for quantifying ubiquitin/proteasome-dependent proteolysis in living cells. Nature Biotechnology, 18(5), 538–543. http://doi.org/10.1038/75406

Davis, P. K., Ho, A., & Dowdy, S. F. (2001). Biological methods for cell-cycle synchronization of mammalian cells. BioTechniques, 30(6), 1322–1326, 1328, 1330–1331.

Feldman, M., & Yagil, G. (1969). Does cycloheximide interfere with protein degradation? Biochemical and Biophysical Research Communications, 37(2), 198–203. http://doi.org/10.1016/0006-291X(69)90719-0

Grillari, J., Katinger, H., & Voglauer, R. (2006). Aging and the ubiquitinome: traditional and non-traditional functions of ubiquitin in aging cells and tissues. Experimental Gerontology, 41(11), 1067–1079. http://doi.org/10.1016/j.exger.2006.07.003

Johnson, E. S., Bartel, B., Seufert, W., & Varshavsky, A. (1992). Ubiquitin as a

degradation signal. The EMBO Journal, 11(2), 497–505.

Johnson, E. S., Ma, P. C., Ota, I. M., & Varshavsky, A. (1995). A proteolytic pathway that recognizes ubiquitin as a degradation signal. The Journal of Biological Chemistry, 270(29), 17442–17456.

Kraft, C., Peter, M., & Hofmann, K. (2010). Selective autophagy: ubiquitin-mediated recognition and beyond. Nature Cell Biology, 12(9), 836–841. http://doi.org/10.1038/ncb0910-836

López-Otín, C., Blasco, M. A., Partridge, L., Serrano, M., & Kroemer, G. (2013). The Hallmarks of Aging. Cell, 153(6), 1194–1217. http://doi.org/10.1016/j.cell.2013.05.039

Mogk, A., Schmidt, R., & Bukau, B. (2007). The N-end rule pathway for proteolysis: prokaryotic and eukaryotic strategies. Trends in Cell Biology, 17(4), 165–172. http://doi.org/10.1016/j.tcb.2007.02.001

Niccoli, T., & Partridge, L. (2012). Ageing as a Risk Factor for Disease. Current Biology, 22(17), R741–R752. http://doi.org/10.1016/j.cub.2012.07.024

Peth, A., Uchiki, T., & Goldberg, A. L. (2010). ATP-dependent steps in the binding of ubiquitin conjugates to the 26S proteasome that commit to degradation. Molecular Cell, 40(4), 671–681. http://doi.org/10.1016/j.molcel.2010.11.002

Pickering, A. M., Lehr, M., Kohler, W. J., Han, M. L., & Miller, R. A. (2015). Fibroblasts From Longer-Lived Species of Primates, Rodents, Bats, Carnivores, and Birds Resist Protein Damage. The Journals of

Gerontology. Series A, Biological Sciences and Medical Sciences, 70(7), 791–799. http://doi.org/10.1093/gerona/glu115

Powers, E. T., Morimoto, R. I., Dillin, A., Kelly, J. W., & Balch, W. E. (2009). Biological and chemical approaches to diseases of proteostasis deficiency. Annual Review of Biochemistry, 78, 959–991. http://doi.org/10.1146/annurev.biochem.052308.114844

Pride, H., Yu, Z., Sunchu, B., Mochnick, J., Coles, A., Zhang, Y., … Pérez, V. I. (2015). Long-lived species have improved proteostasis compared to phylogenetically-related shorter-lived species. Biochemical and Biophysical Research Communications, 457(4), 669–675. http://doi.org/10.1016/j.bbrc.2015.01.046

Rodriguez, K. A., Edrey, Y. H., Osmulski, P., Gaczynska, M., & Buffenstein, R. (2012). Altered Composition of Liver Proteasome Assemblies Contributes to Enhanced Proteasome Activity in the Exceptionally Long-Lived Naked Mole-Rat. PLoS ONE, 7(5), e35890. http://doi.org/10.1371/journal.pone.0035890

Santiago-Josefat, B., Pozo-Guisado, E., Mulero-Navarro, S., & Fernandez-Salguero, P. M. (2001). Proteasome inhibition induces nuclear translocation and transcriptional activation of the dioxin receptor in mouse embryo primary fibroblasts in the absence of xenobiotics. Molecular and Cellular Biology, 21(5), 1700–1709. http://doi.org/10.1128/MCB.21.5.1700-1709.2001

Tanaka, K. (2013). The proteasome: from basic mechanisms to emerging roles.

The Keio Journal of Medicine, 62(1), 1–12.

Treusch, S., Cyr, D. M., & Lindquist, S. (2009). Amyloid deposits: protection against toxic protein species? Cell Cycle (Georgetown, Tex.), 8(11), 1668–1674.

Vabulas, R. M., Raychaudhuri, S., Hayer-Hartl, M., & Hartl, F. U. (n.d.). Protein Folding in the Cytoplasm and the Heat Shock Response. Retrieved September 1, 2015, from http://cshperspectives.cshlp.org

Zhang, L., Gurskaya, N. G., Merzlyak, E. M., Staroverov, D. B., Mudrik, N. N., Samarkina, O. N., … Lukyanov, K. A. (2007). Method for real-time monitoring of protein degradation at the single cell level. BioTechniques, 42(4), 446, 448, 450.